Available online at www.sciencedirect.com

ScienceDirect

Thin Solid Films 516 (2008) 6829 – 6833

thin solid films

www.elsevier.com/locate/tsf

Modeling and experiments of high-pressure VHF SiH_4/H_2 discharges for higher microcrystalline silicon deposition rate ☆

X.D. Zhang [a], F.R. Zhang [a], E. Amanatides [b], D. Mataras [b,*], Y. Zhao [a]

[a] *Institute of photo-electronics thin film devices and technique of Nankai University, Tianjin, 300071, China*
[b] *Plasma Technology Laboratory, Department of Chemical Engineering, Patras University, Patra, 26500, Greece*

Available online 15 December 2007

Abstract

The effect of the total gas pressure (1–3 Torr) on the growth rate and the crystalline volume fraction (Xc) of films deposited from 70 MHz SiH_4/H_2 plasmas is investigated. The films were grown in conditions near the transition from microcrystalline to amorphous silicon growth at high deposition rates (10 Å/s). Simultaneously, a two-dimensional self-consistent fluid model of diluted SiH_4 in H_2 discharges was used to simulate the deposition process. The model integrates a detailed gas phase and surface chemistry including 25 species, 85 gas phase reactions and 27 surface reactions. A good agreement was found between model and experiments concerning the deposition rate. On this basis, the effects of pressure on the electron density and temperature, discharge impedance, electric field distribution as well as on the distribution and importance of the films precursors is discussed.
© 2007 Elsevier B.V. All rights reserved.

Keywords: Plasma enhanced chemical vapor deposition; Microcrystalline silicon; Simulation; High rates

1. Introduction

Hydrogenated microcrystalline silicon (μc–Si:H), deposited by very high frequency plasma-enhanced chemical vapor deposition (VHF–PECVD) from highly diluted silane in hydrogen, is a promising material for the next generation of stable, large area and high efficiency thin film solar cells[1–3]. A major drawback in this direction is the lower light absorption of this material compared to hydrogenated amorphous silicon (a–Si:H), which may be solved by depositing thicker μc–Si:H layers. Therefore, high deposition rates over large areas are a prerequisite for a cost effective industrial application of μc–Si:H solar cells. However, although the material and the deposition process are compatible with the well established a–Si:H technology, there are still several unsolved issues concerning the deposition of device grade materials and high growth rates [4–6]. Among the many process parameters that can play a role in the deposition of μc–Si:H films from SiH_4/H_2 discharges, the total gas pressure and the excitation frequency were identified as having important effects on the deposition rate and were used separately to optimize the process. Recently, a combination of VHF–PECVD with high working pressures [7–9] has been used to explore the possibility of further increasing the deposition rate.

In this paper, we present the effect of the total gas pressure on the deposition rate and the structure of the films deposited from 70 MHz SiH_4/H_2 glow discharges using relatively high power conditions (65 W). The experimental results reveal an optimum pressure for the deposition rate, a continuous drop of the crystalline volume fraction and finally a transition to a–Si:H deposition with pressure. In order to understand the effect of pressure on the deposition process a 2D self-consistent simulation of SiH_4/H_2 discharges was implemented [10,11]. The model results concerning the variation of the discharge electrical parameters, the species' production and the distribution of film precursors with pressure are presented and discussed.

☆ All the authors confirm that the work presented here is original, unpublished and not being considered elsewhere.

* Corresponding author. Plasma Technology Laboratory, Department of Chemical Engineering, University of Patras, P.O. Box 1407, Patras 26504, Greece. Tel.: +30 2610969525; fax: +30 2610993361.
E-mail address: dim@plasmatech.gr (D. Mataras).

0040-6090/$ - see front matter © 2007 Elsevier B.V. All rights reserved.
doi:10.1016/j.tsf.2007.12.066

2. Experimental details

All samples were prepared in a multi-chamber PECVD reactor having an electrode area of 225 cm^2 and an interelectrode distance of 10 mm. The grounded electrode is the substrate holder suitable for 10×10 cm^2 substrates. The details for the system setup can be found in Ref. [12]. The experiments were performed with constant silane concentration (7% in hydrogen) and constant input power (65 W). In this series of experiments, relatively high flow rates (300 sccm) were maintained while the total gas pressure was varied from 133 Pa to 400 Pa. Films of equal thickness (~800 nm) were deposited on corning 7059 glass at a substrate temperature of 200 °C. The structural properties of the samples were characterized with Raman spectroscopy (MKI Renishaw 2000), while the thickness of the thin films was measured with an XP-2 step profiler (AMBios).

3. Plasma simulation

A two dimensional (2D), time dependent fluid model was used to study the deposition of μc–Si:H thin films in the VHF SiH_4/H_2 plasmas. The model describes the discharge using a combination of particle, momentum and electron energy conservation equations derived from the Boltzmann equation, coupled with Poisson's equation for a self-consistent calculation of the electric field. A detailed description of the model can be found in Ref. [13]. A set of 25 species together with a total number of 112 reactions (85 in the gas phase and 27 surface gas interactions) are included into this version of the model, comprising electron-impact reactions with molecular species, neutral-neutral, and ion-neutral reactions. Cross section data are used for the electron impact reactions, whereas the rate constants of the rest of the reactions involving neutral species are either calculated or experimentally measured. Plasma surface interactions of the radicals leading to the growth of μc–Si:H are handled using sticking coefficients.

The input data in this model besides the general process conditions are the geometry of the reactor and the applied voltage while the results include all the important properties of SiH_4/H_2 discharges, like the distribution of the electric field and voltage in the plasma, electron, ion and species densities, electron temperature, radical fluxes towards the substrate and the deposition rate.

4. Results and discussion

Fig. 1 presents Raman spectra of the films deposited at different total gas pressures. The increase of the total gas pressure leads to a decrease of the crystalline volume fraction (Xc) of the material. The intensity of the broad amorphous peak at 480 cm^{-1} is enhanced at higher pressures on cost of the crystalline peak at 520 cm^{-1}, which disappears for a total gas pressure ≥400 Pa. A small shoulder is observed at long wavenumbers for the films prepared at 333 Pa, indicating a transition to a–Si:H growth.

Fig. 1 (b) summarizes both the experimental measurements and the model prediction of the deposition rate as a function of the gas pressure. The experimental results indicate that there is an optimum of the film growth rate for the pressure of 267 Pa. On the other hand the model predicts that the deposition rates increases linearly with the pressure. For the pressure range 133 Pa to 267 Pa (μc–Si:H window) the trend is exactly the same for both experimental and simulation results while the simulation overestimates slightly the film growth rate mainly because it does not take into account powder formation, which was obvious at the specific experimental conditions. The differences observed for pressures higher than 267 Pa (a–Si:H deposition), are due to the fact that the model uses a specific surface reaction set that is valid only for the deposition of μc–Si:H. This is because μc–Si:H and a–Si:H growth mechanisms are different; the radicals and especially silyl (SiH_3) have different probabilities to interact with a–Si:H or μc–Si:H surfaces, while also the reactions rates between the surface sites are rather different. In the study presented here, no further effort was made to incorporate the a–Si:H growth model. Thus, the discussion below is limited to the study of the pressure effect on the microcrystalline silicon deposition regime.

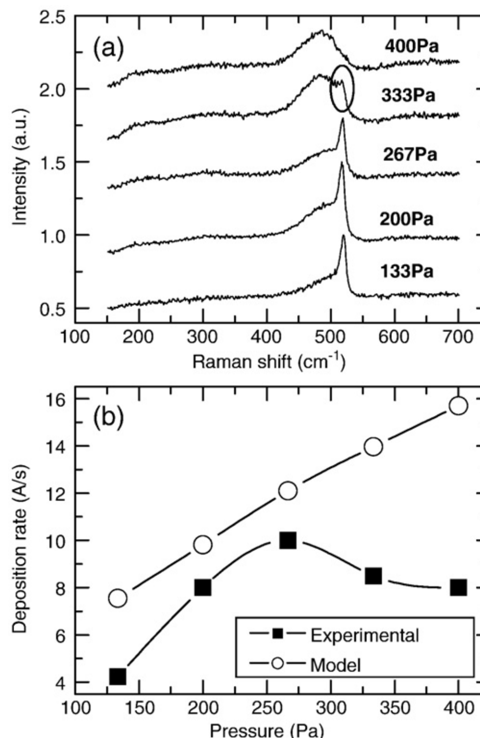

Fig. 1. (a) Raman spectra of the deposited films and (b) experimental and simulation results of the deposition rate as a function of the total gas pressure.

Following the examination of the level and range of agreement between the model and the experimental results, the model was used to understand the important changes induced by the increase of pressure in both the film growth rate and crystallinity. For this purpose, the model results concerning plasma microscopic parameters and gas-phase species production were thoroughly analyzed. Thus, Fig. 2 presents the variation of the time and space averaged electron density (N_e, left axis) and electron temperature (T_e, right axis) as a function of the total gas pressure. The model predicts a significant increase of N_e by a

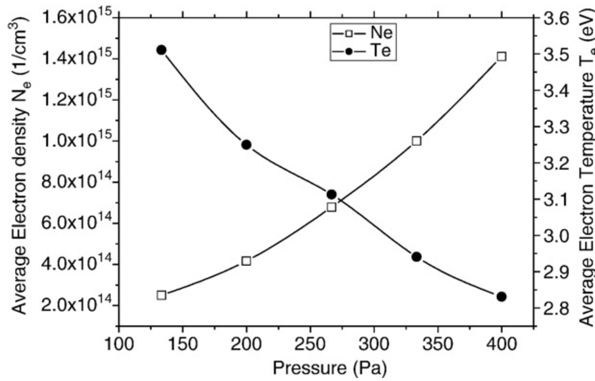

Fig. 2. Simulation results for the time and space averaged electron density (N_e) (left axis) and electron temperature (T_e) (right axis), as a function of pressure.

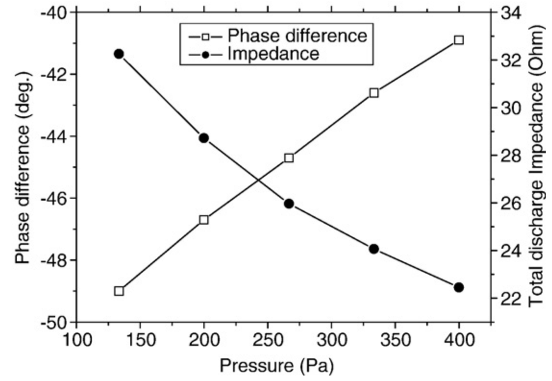

Fig. 4. Discharge phase difference (left axis) and total impedance (right axis) as a function of pressure.

factor of 7 and simultaneously a drop of T_e with pressure. These results can be explained by the reduction of charged species losses to the surfaces due to the decrease of both electron and ion mobilities with pressure as well as by the variation of the real power dissipated in the discharge [14]. In this specific set of experiments the generator power was maintained constant (65 W) and this leads to a variation of the power actually dissipated in the discharge due to a change in the plasma impedance. Namely, Fig. 3 (left axis) reflects the changes in the coupling between the generator and the plasma by presenting the change of the real power consumed in the discharge as a function of the total gas pressure. The results indicate that the larger the gas density the better the % power transferred from the generator to the plasma. This has been also experimentally confirmed since for the same generator input the voltage measured at the RF electrode increased with pressure. The increase of the real power consumed in the discharge is then responsible for the higher electron density presented in Fig. 1 as the number of ionization events would be enhanced at higher pressures. In turn, the increase of electron density will be responsible for the higher current conduction, which is also presented in Fig. 2 (right axis). Actually, discharge power and discharge current have exactly the same trend with pressure, because in these conditions power dissipation is mainly determined by electrons — heating and collisions in the bulk of the plasma rather than in the high field sheaths. This is typical for VHF discharges which are characterized by the application of low voltages with a subsequent enhancement of bulk heating.

The above discussion is further supported by the calculated values of the discharge phase and impedance as presented in Fig. 4. Thus, despite the significant increase in the discharge power and the significant variation of the gas density, the change in the discharge phase and impedance with pressure is relatively small. This means that a large number of electrons and especially the electrons with relatively low energy suffer very few or even no momentum transfer or inelastic collisions during the short period of 70 MHz excitation. Thus, the prospective increase of the discharge ohmic character is not as strong as in the case of lower frequency (13.56 MHz) discharges.

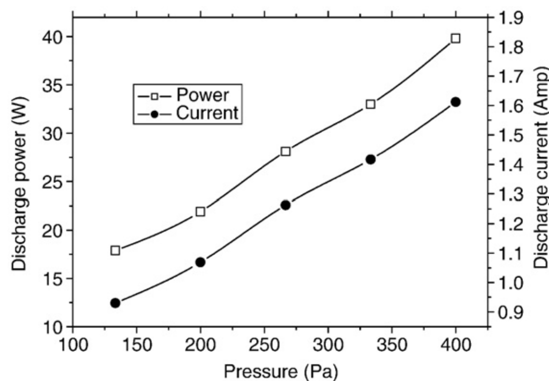

Fig. 3. Model prediction for the total discharge power (left axis) and the total discharge current as a function of pressure.

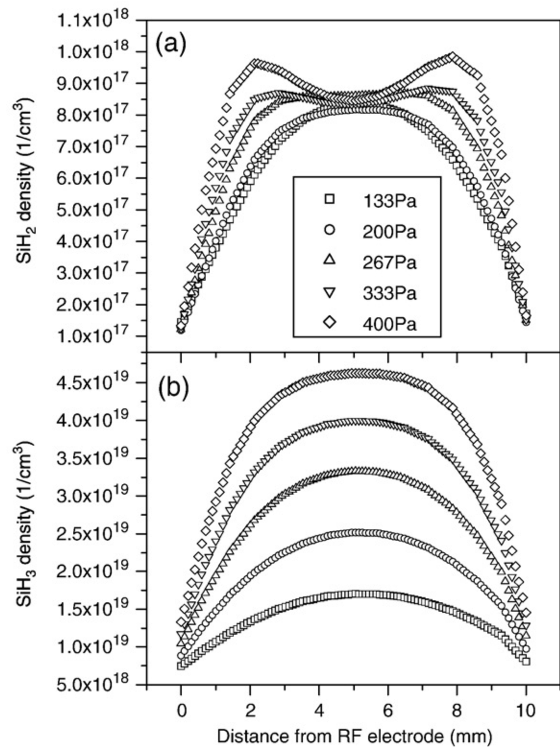

Fig. 5. Spatial distribution of (a) SiH_2 and (b) SiH_3 radical densities for different pressures.

The changes predicted for the electrical parameters of the discharge (power, plasma conductivity, electron temperature) affects also the gas-phase chemistry mainly through electron-molecule collisions. Thus, Fig. 5 shows the spatial distribution of silylene (SiH_2) and silyl (SiH_3) species that are initially produced through electron impact dissociation of SiH_4 and are the dominant silicon hydrides for these conditions. The steady state distribution of these species in the discharge is the result of their production in the gas phase, their consumption in the gas phase and the surface and their mass transport (diffusion-dominated in these conditions). It is evident that SiH_3 and SiH_2 radicals have different spatial distribution shapes because of their different-gas phase and surface reactivities. Concerning SiH_3 radicals the increase of pressure results in an enhancement of their density everywhere in the discharge. This enhancement is due to the increase of power dissipation and consequently the enhancement of electron impact SiH_4 dissociation rate and also due to the increase of SiH_4 density in the discharge as the mole fraction of SiH_4 in the gas mixture was kept constant (7%). On the other hand, the distribution of SiH_3 in the discharge does not change and it is in all cases of a bell shape with a maximum in the center of the plasma. This is a typical distribution for species with diffusion dominated mass transport and consumption determined by their surface reactions. On the other hand, for the SiH_2 radicals, the increase of pressure leads to a slight increase of their density, because of the competitive increase of their production and consumption rates in the gas phase through the enhancement of secondary gas phase reactions with SiH_4. The latter is also responsible for the distribution change of SiH_2 at pressures higher than 333 Pa as a large number of SiH_2 species that are produced are spontaneously consumed. So at these pressures the profile of these species is mainly determined by their production and consumption in the gas phase rather than from their mass transport or their consumption at the growing film surface.

It is worth mentioning that H atoms, which are also very important species for the microcrystalline silicon growth, have a similar behavior with SiH_2 i.e. their density and distribution in space are increasingly affected by the insertion reaction with SiH_4 as pressure increases. This can be observed in Fig. 6 which presents the spatial distribution of H atoms for different gas pressures where it seems that for pressures higher than 267 Pa the distribution of the species is mainly determined by their gas phase consumption. Thus, although H_2 density in the plasma increases by a factor of 3 when increasing pressure from 133 to 400 Pa, H atom density increases only by a factor of 1.2 whereas SiH_3 density is enhanced by a factor of 2.8. These observations lead to the conclusion that as we shift from the conditions of μc–Si:H growth to conditions of a–Si:H growth a relative change of the relative importance of the film precursors take place. In fact, in conditions of a–Si:H deposition the silyl radical seems to dominate the film growth while the role of highly reactive in the gas phase radicals and also of H atoms is increasingly constrained.

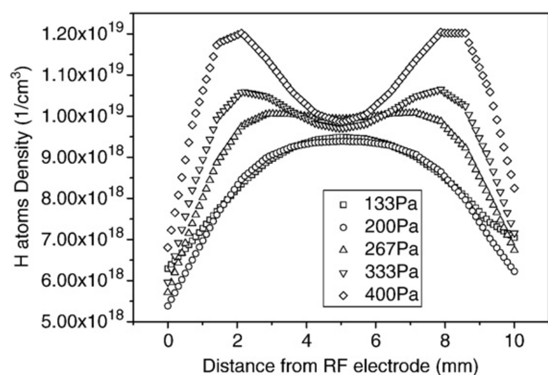

Fig. 6. Spatial distribution of H atom density for different gas pressures.

5. Conclusions

The effect of total gas pressure (133–400 Pa) on the growth rate and the crystalline volume fraction (Xc) of silicon films deposited from 70 MHz 7% SiH_4 in H_2 discharges was investigated. An optimum of the deposition rate at 267 Pa and a transition to a–Si:H deposition at 333 Pa was found.

At the same time, a two-dimensional self-consistent model of diluted SiH_4 in H_2 discharges was implemented for the simulation of the deposition process and for understanding the complex effects of the total gas pressure on the discharge properties that finally lead to the transition from μc–Si:H to a–Si:H growth.

The model predicted that for the same generator power (65 W) the increase of pressure resulted to a continuous enhancement of the real power dissipated in the discharge with a consequent increase of plasma density and conductivity. At the same time a small drop of the discharge impedance and the mean electron temperature was calculated. These changes were attributed to the application of VHF frequency and the small number of collisions that the electrons suffered during the short period of the VHF cycle.

Finally, the simulation results concerning the species' production and distribution in the discharge have shown that the increase of pressure favors the role of silyl radicals in the film growth relative to species as SiH_2 and H, which have rather high gas phase reactivity. Taking into account that at pressures higher than 333 Pa a transition to a–Si:H deposition was observed, we conclude that these changes lead to the transition.

Acknowledgements

Project supported by National Natural Science Foundation of China (60506003), International cooperation project between China–Greece Governments, the State Key Development Program for Basic Research of China (Grant No.2006CB202 600), Natural Science Foundation of Tianjin of China (05YFJ MJC01600), the starting project of Nankai University (J02031), and the Program for New Century Excellent Talents in University of China (NCET). Two of the authors (E. Amanatides and D. Mataras) wish also to thank the European Social Fund (ESF) Operational Program for Educational and Vocational Training II EPEAEK II, and particularly the Program PYTHAGORAS for partly funding this work.

References

[1] O. Vetterl, A. lamberts, A. Dasgupta, F. Finger, B. Rech, O. Kluth, H. Wagner, Sol. Energy. Mater. Sol. Cells 66 (2001) 345.
[2] J. Meier, E. Vallat-Sauvain, S. Dubail, U. Kroll, J. Dubail, S. Golay, L. Feitknecht, P. Torrs, S. Fay, D. Fischer, A. Shah, Sol. Energy. Mater. Sol. Cells 66 (2001) 73.
[3] K. Yamamoto, M. Yoshimi, T. Suzuki, Y. Tawada, Y. Okamoto, A. Nakajima, Mater. Res. Soc. Symp. Proc. 507 (1998) 131.
[4] A. Matsuda, J. Non-Cryst. Solids 59-60 (1983) 767.
[5] S. Vepřek, F.-A. Sarrot, S. Rambert, E. Taglauer, J. Vac. Sci. Technol. A 7 (1989) 2614.
[6] J. Meier, R. Fluckiger, H. Keppner, A. Shah, Appl. Phys. Lett. 65 (1994) 860.
[7] M. Fukawa, S. Suzuki, L. Guo, A. Matsuda, Sol. Energy Mater. Sol. Cells 66 (2001) 217.
[8] J.K. Rath, R.H.J. Franken, A. Gordijn, R.E. Schropp, W.J. Goedheer, J. Non-Cryst. Solids 338-340 (2004) 56.
[9] U. Graf, J. Meier, U. Kroll, J. Bailat, C. Droz, E. Vallat-Sauvain, A. Shah, Thin Solid Films 427 (2003) 37.
[10] M.J. Kushner, J. Appl. Phys. 63 (1988) 2532.
[11] G.J. Nienhuis, W.J. Goedheer, E.A.G. Hamers, W.G.J.H.M. van Stark, J. Bezemer, J. Appl. Phys. 82 (1997) 2060.
[12] Y. Zhao, X.D. Zhang, F. Zhu, Y.T. Gao, C.C. Wei, J.M. Xue, H.Z. Ren, D.K. Zhang, G.F. Hou, J. Sun, X.H. Geng, 15th International Photovoltaic Science & Engineering Conference , 10-15 Oct. 2005, Shanghai, China, vol. 65, 2005.
[13] B. Lyka, E. Amanatides, D. Mataras, 19th European Photovoltaic Solar Energy Conference, 7-11 June 2004, Paris, France, vol. 1395, 2004.
[14] E. Amanatides, D. Mataras, J. Appl. Phys. 89 (2001) 1556.